

Accepted Manuscript

Design of a water soluble 1,8-naphthalimide/3-hydroxy-4-pyridinone conjugate: investigation of its spectroscopic properties at variable pH and in the presence of Fe³⁺, Cu²⁺ and Zn²⁺

Tânia Moniz, Carla Queirós, Rita Ferreira, Andreia Leite, Paula Gameiro, Ana M.G. Silva, Maria Rangel

PII: S0143-7208(13)00070-3

DOI: [10.1016/j.dyepig.2013.02.020](https://doi.org/10.1016/j.dyepig.2013.02.020)

Reference: DYPI 3867

To appear in: *Dyes and Pigments*

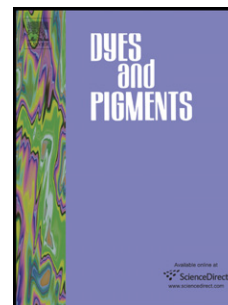
Received Date: 9 January 2013

Revised Date: 22 February 2013

Accepted Date: 25 February 2013

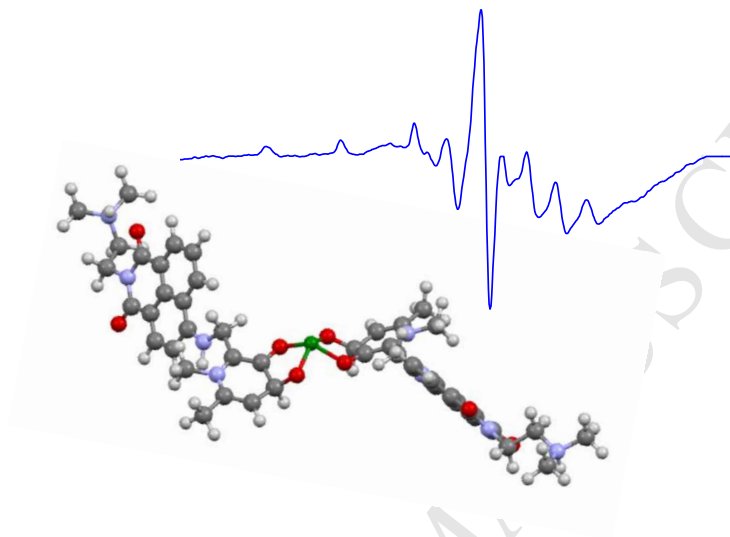
Please cite this article as: Moniz, T, Queirós, C, Ferreira, R, Leite, A, Gameiro, P, Silva, AMG, Rangel M, Design of a water soluble 1,8-naphthalimide/3-hydroxy-4-pyridinone conjugate: investigation of its spectroscopic properties at variable pH and in the presence of Fe³⁺, Cu²⁺ and Zn²⁺, *Dyes and Pigments* (2013), doi: 10.1016/j.dyepig.2013.02.020.

This is a PDF file of an unedited manuscript that has been accepted for publication. As a service to our customers we are providing this early version of the manuscript. The manuscript will undergo copyediting, typesetting, and review of the resulting proof before it is published in its final form. Please note that during the production process errors may be discovered which could affect the content, and all legal disclaimers that apply to the journal pertain.



Design of a water soluble 1,8-naphthalimide/3-hydroxy-4-pyridinone conjugate: investigation of its spectroscopic properties at variable pH and in the presence of Fe^{3+} , Cu^{2+} and Zn^{2+}

Tânia Moniz, Carla Queirós, Rita Ferreira, Andreia Leite, Paula Gameiro, Ana M.G. Silva and Maria Rangel



Design of a water soluble 1,8-naphthalimide/3-hydroxy-4-pyridinone conjugate: investigation of its spectroscopic properties at variable pH and in the presence of Fe³⁺, Cu²⁺ and Zn²⁺

Tânia Moniz,^a Carla Queirós,^a Rita Ferreira,^a Andreia Leite,^a Paula Gameiro,^a Ana M.G. Silva,^{a*} and Maria Rangel^{b*}

^a *REQUIMTE, Departamento de Química e Bioquímica, Faculdade de Ciências, Universidade do Porto, 4169-007 Porto, Portugal*

^b *REQUIMTE, Instituto de Ciências Biomédicas Abel Salazar, Universidade do Porto, 4099-003 Porto, Portugal*
**mcrangel@fc.up.pt; ana.silva@fc.up.pt*

Abstract

The synthesis and sensing properties of a new fluorescent probe designed to have a 4-amino-1,8-naphthalimide fluorescent platform functionalized with a 3-hydroxy-4-pyridinone bidentate chelating unit at the 4-position and a terminal aliphatic dimethylamino group at the imide site, are reported. The absorption and fluorescence properties of the ligand were investigated in DMSO and in aqueous solution at variable pH and in the presence of increasing concentration of Fe³⁺, Cu²⁺ and Zn²⁺.

Analysis of the UV-Vis spectra at variable pH allowed the determination of three p*K_a* values (p*K_{a1}* = 3.19, p*K_{a2}* = 8.38, p*K_{a3}* = 9.95) and establishment of the corresponding speciation diagram. Fluorescence spectra obtained in the same conditions show that the fluorescence intensity of the probe decreases with increasing pH and are *off* above pH 9 as a result of photo-induced electron transfer arising from the aliphatic dimethylamino group. Under physiological pH conditions, the probe shows an absorption band centred at 439 nm and emits in the green at λ = 536 nm.

Analysis of UV-Vis and EPR spectra of the ligand in the presence of Fe³⁺ and Cu²⁺ is consistent with the formation of the corresponding metal ion complexes. The fluorescence intensity of the ligand is quenched in the presence of variable concentrations of Fe³⁺, Cu²⁺ and Zn²⁺ and under physiological pH conditions the fluorescence of the probe is *ca* 92%, 88% and 91% quenched in the presence of Fe³⁺, Cu²⁺ and Zn²⁺ respectively.

Keywords

4-amino-1,8-naphthalimides, 3-hydroxy-4-pyridinones, microwave-assisted synthesis, fluorescence properties

Introduction

Since the early reports by Tsien and co-workers regarding fluorescent probes for calcium,^{1,2} the design of highly efficient fluorescent probes for sensing and monitoring various chemical species has received an increasing interest from the scientific and industrial communities. Indeed, many fluorescent probes have been developed for different applications including probes sensitive to pH,³ to metal ions,⁴ to monitor enzymatic activity,⁵ reactive oxygen and nitrogen species (ROS and RNS)⁶ and many other analytes.⁷

The most general design concept of fluorescent metal ion probes involves the use of the photoinduced electron transfer (PET) model based on the covalent linkage of a single or branched chelating architecture and a fluorophore unit. The covalent linkage which separates the two units is typically a short aliphatic spacer that minimizes any ground-state interactions. In these probes, the interaction with the analyte will cause significant changes in the emission spectra accompanied by no, or minor, changes in the absorption spectra of the probes.⁸

Originally detailed by de Silva et al.^{9a,b} and Czarnik et al.,^{9c,d} this process has been widely used in the construction of many fluorescent probes, with special emphasis for 4-amino-1,8-naphthalimide based fluorescent probes.¹⁰

4-Amino-1,8-naphthalimides are fluorophores that exhibit bands with an ICT (intramolecular charge transfer) character caused by the electronic conjugation of the electron donating amine and the electron withdrawing imide (Fig. 1).¹¹ The ICT character gives rise to a large excited-state dipole and broad absorption and emission bands typically centred at *ca* 450 and 550 nm, respectively, when recorded in water.¹⁰ The spectroscopic properties of 4-amino-1,8-naphthalimides are also highly solvent dependent, noting that polar protic solvents stabilize the ICT character more than apolar solvents. The compounds have fairly simple structures for which facile and straightforward synthetic methods have been established and their structure allows changes on either the amine function in the 4-position of the aromatic naphthalene moiety, or at the imide nitrogen atom.¹² Consequently, the 4-amino-1,8-naphthalimides have been extensively used as strongly absorbing and colorful fluorophores in the design of

fluorescent probes, particularly for sensing biologically relevant metal ions, such as Cu^{2+} and Zn^{2+} ,¹³ and heavy metal ions, like Hg^{2+} and Pd^{2+} .¹⁴

In most examples, 4-bromo-1,8-naphthalimide, which is a very weak fluorescent compound, has been used as precursor to reach a variety of metal sensing fluorescent probes based on the 4-amino-1,8-naphthalimide platform. These fluorescent probes have been synthesized using mainly two synthetic strategies: (i) direct nucleophilic displacement of the bromine atom of the 4-bromo-1,8-naphthalimide with a functional amine or (ii) initial reaction with a linker and subsequent introduction of the functional moiety. These synthetic approaches have been chosen for the design of many metal sensing fluorescent probes where, in most instances, the nitrogen atom introduced in position 4 of the naphthalimide molecule can be involved in metal ion coordination.¹⁵

Hydroxypyridinones are an important class of *N*-heterocyclic bidentate chelators which show high affinity towards several biological important metal ions, such as Fe(III).¹⁶ This type of chelator, which include analogues of 1,2-hydroxypyridinone (1,2-HPO), 2,3-hydroxypyridinone (2,3-HPO) and 3,4-hydroxypyridinone (3,4-HPO), have been widely used as decorporation agents for the medical treatment of iron overload associated with several diseases.¹⁷ Also some hydroxypyridonate complexes have been applied as Fe(III) chelators for reducing iron toxicity.¹⁸

Among the different types of hydroxypyridinones, the 3,4-HPO class is particularly attractive for pharmaceutical purposes since their structure allows tailoring of their hydrophilic/lipophilic balance (HLB) without significantly changing its chelating properties.¹⁹ Variations in HLB can be achieved by simply introducing appropriate substituents on the endocyclic nitrogen atom of the pyridinone ring, the 3-hydroxy-4-pyridinones are synthesized by the reaction of 3-hydroxy-4-pyrones with primary amines, thus leading to the optimal lipophilicity for delivery or removal of metal ions in the body.¹⁹

In recent years, many 3,4-HPOs modified with fluorescent platforms, like coumarin or fluorescein, have been developed by the Hider's laboratory. The latter probes have shown to be selective fluorescence quenchers for Fe^{3+} up to 90% and found application in the determination of cellular iron concentrations.²⁰ Lately, Callan et al. summarized the development of various molecular and supramolecular fluorescent sensors that have been successfully used for detection of Fe^{3+} , many of them based on 3,4-HPO derivatives.²¹

Our group has long been interested in the synthesis and solution properties of 3,4-HPO ligands for biomedical applications^{19,22} and more recently on the design of metal ion sensors.²³ Lately, we prepared two bidentate ligands bearing a 3,4-HPO chelator moiety and a naphthalene fluorescent platform that can be used to sense metal ions in organic solvents but due to their very low solubility and lack of fluorescent properties in water are not usable to monitor metal ions in aqueous media.^{23a}

In the present work we report the design and properties of a new 3,4-HPO probe with high solubility in water and suitable fluorescence properties in aqueous solution. In order to achieve our purpose and in view of the well-known properties of 1,8-naphthalimide derivatives we coupled a 3,4-HPO bidentate chelating unit with the 4-amino-1,8-naphthalimide platform (Fig. 2). The chelator backbone is connected to the fluorophore through the *ortho* position relative to one of the chelating oxygen atoms of the 3,4-HPO moiety, thus providing a more rigid structure and a close proximity between the fluorophore and the binding unit. The 1,8-naphthalimide platform was modified at the imide nitrogen atom in order to accommodate a terminal aliphatic amino group that increases solubility in a pH range determined by the pK_a of the amino group. To the best of our knowledge this is the first report of a molecule conjugating the 1,8-naphthalimide platform with a 3-hydroxy-4-pyridinone chelator.

Experimental

Materials and instrumentation

Chemicals were obtained from Sigma–Aldrich (grade puriss, p.a.) and were used as received unless otherwise specified.

Nuclear magnetic resonance spectra (¹H and ¹³C NMR) were measured on a Bruker III Avance 400 spectrometer operating at 400.15 MHz and 100.62 MHz for ¹H and ¹³C spectra, respectively. Chemical shifts (δ) are reported in parts per million and coupling constants (J) in hertz; internal standard was TMS. Unequivocal ¹H assignments were made with aid of 2D gCOSY (¹H/¹H), while ¹³C assignments were made on the basis of 2D gHSQC (¹H/¹³C) and gHMBC experiments (delay for long range J C/H couplings were optimized for 7 Hz). Mass spectrometry analysis were performed at the University of Santiago de Compostela (Spain). Melting points were measured in a glass capillary tube on a Stuart Scientific SMP1 apparatus

and are uncorrected. FTIR spectra were obtained with a Perkin Elmer FT-IR System (Spectrum BX) with ATR (Attenuated Total Reflectance).

Synthesis

Synthesis of *N*-(dimethylamino)ethyl-4-bromo-1,8-naphthalimide (**3**)

Following reported procedures,⁴⁰ a mixture of 4-bromo-1,8-naphthalic anhydride **1** (0.10 g, 0.36 mmol), *N,N*-dimethylethylenediamine **2** (0.05 mL, 0.43 mmol) and ethanol (1 mL) was heated under reflux for 4 hours. After cooling to room temperature (RT), the solid that formed was filtered, washed with water and dried to yield quantitatively naphthalimide **3**. ¹H NMR (400 MHz, CDCl₃) δ: 2.35 (s, 6H, N(CH₃)₂CH₂CH₂-), 2.65 (t, 2H, *J* 7.2 Hz, N(CH₃)₂CH₂CH₂-), 4.32 (t, 2H, *J* 7.2 Hz, N(CH₃)₂CH₂CH₂-), 7.85 (dd, 1H, *J* 8.4 and *J* 7.2 Hz, H-6), 8.05 (d, 1H, *J* 7.8 Hz, H-3), 8.42 (d, 1H, *J* 7.8 Hz, H-2), 8.58 (d, 1H, *J* 8.4 and *J* 0.8 Hz, H-5 or H-7), 8.66 (d, 1H, *J* 7.2 and *J* 0.8 Hz, H-5 or H-7).

Synthesis of *N*-(dimethylamino)ethyl-4-(2'-aminomethyl-1',6'-dimethyl-3'-benzyloxy-4'-pyridinone)-1,8-naphthalimide (**5**)

The procedure to synthesize the compound was adapted from those described in the literature.⁴¹ A pressure vial of 10 mL was charged with naphthalimide **3** (0.130 g, 0.375 mmol), 1,6-dimethyl-2-aminomethyl-3-benzyloxy-4-pyridinone **4**²⁴ (0.194 g, 0.75 mmol), Pd(OAc)₂ (4.2 mg, 0.019 mmol), BINAP (11.8 mg, 0.019 mmol), *t*-BuOK (42.1 mg, 0.375 mmol) and DMF (0.5 mL) and the cap was tightened thoroughly. The vessel was exposed to microwave irradiation at 130°C (1 min ramp to 130°C and 4 min hold at 130°C, using a maximum power of 150 W). The reaction tube was thereafter cooled to RT and the mixture was purified by flash chromatography and preparative TLC using a mixture of chloroform/methanol (9:1). Product **5** was crystallized in chloroform/methanol to give 126.3 mg (64% of yield) of a yellow powder. Mp 205-207 °C. IR (cm⁻¹) 2956 (N-H), 1682, 1646, 1622 (C=O), 1582, 1576, 1554, 1532, 1506, 1456, 1392, 1364, 1326, 1290, 1244, 1222, 1142, 1120, 1098, 1048, 1028, 972, 954, 842, 774, 746, 698. ¹H NMR (400 MHz, CDCl₃) δ: 2.33 (s, 3H, 6'-CH₃), 2.40 (s, 6H, N(CH₃)₂CH₂CH₂-), 2.70 (t, 2H, *J* 7.2 Hz, N(CH₃)₂CH₂CH₂-), 3.56 (s, 3H, 1'-CH₃), 4.27 (d, 2H, *J* 4.0 Hz, HNCH₂), 4.34 (t, 2H, *J* 7.2 Hz, N(CH₃)₂CH₂CH₂-), 5.10 (s, 2H, CH₂C₆H₅), 6.29 (s, 1H, H-5'), 6.53 (d, 1H, *J* 8.4 Hz, H-3), 7.00-7.03 and 7.10-7.13 (2m, 5H, CH₂C₆H₅), 7.61 (dd, 1H, *J* 8.3 and *J* 7.4 Hz, H-6), 8.42 (d, 1H, *J* 8.3 Hz, H-2), 8.51 (d, 1H, *J* 8.3 Hz, H-5 or H-7), 8.56 (d, 1H, *J* 7.4 Hz, H-5 or H-7). ¹³C NMR (100 MHz,

CDCl₃) δ : 20.9 (6'-CH₃), 36.2 (1'-CH₃), 37.8 ($\underline{\text{CH}_2\text{CH}_2\text{N}(\text{CH}_3)_2}$), 39.7 (HNCH₂), 45.7 (N(CH₃)₂CH₂CH₂-), 57.0 (N(CH₃)₂ $\underline{\text{CH}_2\text{CH}_2}$ -), 73.1 ($\underline{\text{CH}_2\text{C}_6\text{H}_5}$), 104.5 (C-3), 111.4 (C-1a), 118.8 (C-5'), 121.2 (C-4a), 122.7 (C-7b), 124.9 (C-6), 128.09 (C-7), 128.2, 128.4, 129.6, 129.7, 131.3, 134.2, 136.6, 139.6 (C-2'), 146.0 (C-3'), 147.9 (C-6'), 149.3, 164.1 (C-1), 164.7 (C-8), 173.4 (C-4'). MS (FAB) m/z : 525 [M+H]⁺. HRMS (FAB) m/z Calcd. for C₃₁H₃₃N₄O₄ 525.2502; Found 525.2501.

Synthesis of *N*-(dimethylamino)ethyl-4-(2'-aminomethyl-1',6'-dimethyl-3'-hydroxy-4'-pyridinone)-1,8-naphthalimide dihydrochloride (N-3,4-HPO)

A 1 M solution of boron trichloride in dichloromethane (1.5 mL) was dropped slowly into an ice-bath-cooled suspension of derivative **5** (106.1 mg, 0.202 mmol) in dry dichloromethane (10 mL), under an argon atmosphere. The mixture was stirred at room temperature for 5 h. Methanol (5 mL) was added to quench the reaction. After removal of the solvent in vacuum, the residue was precipitated with methanol/ acetone to afford the hydrochloride salt of **N-3,4-HPO** (102.6 mg, 73% of yield) isolated as a yellow powder. Mp 213-215 °C. IR (cm⁻¹) 3310 (O-H), 2906 (N-H), 1682, 1634, 1616 (C=O), 1586, 1576, 1538, 1504, 1480, 1392, 1354, 1280, 1248, 1204, 1120, 1102, 1036, 1020, 960, 940, 898, 784, 754, 586. ¹H NMR (400 MHz, DMSO-d₆) δ : 2.57 (s, 3H, 6'-CH₃), 2.87 (d, 6H, *J* 4.0 Hz, ⁺NH(CH₃)₂CH₂CH₂-), 3.40-3.42 (m, 2H, ⁺NH(CH₃)₂ $\underline{\text{CH}_2\text{CH}_2}$ -), 3.97 (s, 3H, 1'-CH₃), 4.35-4.36 (m, 2H, ⁺NH(CH₃)₂CH₂ $\underline{\text{CH}_2}$ -), 4.91 (d, 2H, *J* 3.6 Hz, $\underline{\text{CH}_2\text{NH}}$), 7.01 (d, 1H, *J* 8.6 Hz, H-3), 7.30 (s, 1H, H-5'), 7.73 (dd, 1H, *J* 8.4 and *J* 7.4 Hz, H-6), 8.31 (d, 1H, *J* 8.6 Hz, H-2), 8.48 (d, 1H, *J* 7.4 Hz, H-7), 8.75 (br. s, 2H, OH), 8.92 (d, 1H, *J* 8.4 Hz, H-5) 9.97 (br. s, 1H, ⁺NH(CH₃)₂CH₂CH₂-). ¹³C NMR (100 MHz, DMSO-d₆) δ : 20.8 (6'-CH₃), 34.8 (⁺NH(CH₃)₂CH₂ $\underline{\text{CH}_2}$ -), 38.5 (HNCH₂), 40.0 (1'-CH₃, under DMSO signal), 42.6 (⁺NH($\underline{\text{CH}_3}$)₂CH₂CH₂-), 54.8 (⁺NH(CH₃)₂ $\underline{\text{CH}_2\text{CH}_2}$ -), 104.4 (C-3), 109.2, 112.7 (C-5'), 120.5 (C-7b), 122.0, 124.8 (C-6), 128.5, 129.4 (C-5), 130.9 (C-7), 134.1 (C-2), 139.1 (C-2'), 143.2 (C-3'), 148.6 (C-6'), 149.1, 150.0 (C-4), 160.0 (C-4'), 163.3 (C-1), 164.3 (C-8). ¹H NMR (400 MHz, D₂O+DCl) δ : 2.55 (s, 3H, 6'-CH₃), 2.94 (s, 6H, ⁺NH($\underline{\text{CH}_3}$)₂CH₂CH₂-), 3.33 (m, 2H, ⁺NH(CH₃)₂ $\underline{\text{CH}_2\text{CH}_2}$ -), 3.98 (s, 3H, 1'-CH₃), 4.18 (m, 2H, ⁺NH(CH₃)₂CH₂ $\underline{\text{CH}_2}$ -), 4.80 (s, 2H, $\underline{\text{CH}_2\text{NH}}$), 6.52 (m, 1H, H-3), 7.12 (s, 1H, H-5'), 7.32 (m, 1H, H-6), 7.69 (m, 1H, H-2), 7.91 and 8.01 (2m, 2H, H-5 and H-7). ¹³C NMR (100 MHz, D₂O+DCl) δ : 21.4 (6'-CH₃), 36.0 (⁺NH(CH₃)₂CH₂ $\underline{\text{CH}_2}$ -), 39.4 (HNCH₂), 40.0 (1'-CH₃), 44.3 (⁺NH($\underline{\text{CH}_3}$)₂CH₂CH₂-), 56.4 (⁺NH(CH₃)₂ $\underline{\text{CH}_2\text{CH}_2}$ -), 105.6 (C-3), 108.8, 114.1 (C-5'), 120.5, 120.9, 125.7 (C-6), 129.3 (C-5 or C-7), 129.7, 132.2 (C-5 or C-7), 135.3 (C-2), 139.1, 143.8 (C-3'), 151.2, 151.6, 160.0 (C-

4'), 165.2 (C-1 or C-8), 166.1 (C-1 or C-8). MS (ESI) m/z 435 $[M+H]^+$. HRMS (ESI) m/z Calcd. for $C_{24}H_{27}N_4O_4$ 435.2044; Found 435.2027.

Absorption and Fluorescence spectroscopic measurements

Absorption spectra were acquired with a Perkin Elmer Lambda 25 spectrophotometer equipped with a constant-temperature cell holder, at 25°C, in 1 cm cuvettes, in the wavelength range 225–650 nm.

Fluorescence measurements were performed in a Varian Cary Eclipse fluorometer, equipped with a constant-temperature cell holder, at 25°C, in 1 cm cuvettes.

Stock solutions of the different compounds were obtained by preparing a concentrated solution of the compound in dimethylsulfoxide (DMSO). Samples for absorption and fluorescence measurements were prepared by dilution of the appropriate volume of the DMSO stock solution. The percentage of the DMSO stock solution in the final volume of the MOPS buffer solutions was always less than 1%.

Quantum yield determination

The fluorescence quantum yield values for 1,8-naphthalic anhydride (**1**) and **N-3,4-HPO** and 5(6)-carboxyfluorescein were determined, at 25°C, according to the method of Williams *et al.*³⁰ and what is described by Fery-Forgues and Lavabre,⁴² using fluorescein as standard.³¹ To minimize reabsorption effects, the absorbance's sample values were kept below 0.1.

Absorption and fluorescence spectra of N-3,4-HPO at variable pH

The characterization in aqueous solution was performed at 25°C and at variable pH. For variable pH measurements we started from a solution prepared as previously described and aliquots of strong acid or base were added to adjust pH to the desired value. After each pH adjustment the solution was transferred into the cuvette, and the absorption spectra were recorded. Spectra were acquired at 25°C and between 225 and 800 nm (1 nm resolution).

For the spectroscopic data the pH values were measured with a Crison pH meter Basic 20+ which is equipped with a combined glass electrode, and standardized at 25°C using standard buffers of pH 4, 7 and 9. The UV-Vis spectra obtained to determine pK_a values were recorded, at each pH, using a Varian Cary bio50 double beam spectrophotometer, equipped with a Varian Cary single cell Peltier accessory controlled by a computer. The pK_a values were calculated using the program HypSpec.³⁴ The errors reported in this work were

calculated by the method suggested by Albert and Sarjeant.⁴³ The distribution diagrams were plotted with the program HySS 2008.⁴⁴

Fluorescence spectra at variable pH were obtained using several buffers and considering the concentration requirements for fluorescence spectroscopy.

Evaluation of the interaction of the probe N-3,4-HPO with Fe³⁺, Cu²⁺ and Zn²⁺

The evaluation of the interaction of probe **N-3,4-HPO** with metal ions was performed in DMSO and in MOPS buffer (pH 7.4, I=0.1 M NaCl) at 25°C. Stock solutions of the different metal ions were acquired [Fe(NO₃)₃, Cu(NO₃)₂ and Zn(NO₃)₂] from Sigma-Aldrich and stabilized with nitrilotriacetic acid trisodium salt (NTA) at a 1:5 proportion. Concentrated solutions of **N-3,4-HPO** in DMSO were prepared and used as stock solutions. To prepare the solution for fluorescence measurements, a known volume of **N-3,4-HPO** was diluted with MOPS buffer to achieve a final concentration of, approximately, 3 μM. Increasing amounts of the metal stock solutions were added to the 3 μM solution of the probe **N-3,4-HPO**, in a range of molar ratios from 1:0.01 to 1:1 (chelator:metal ion).

The UV-Vis spectra were recorded after each addition using a Varian Cary bio50 double beam spectrophotometer, equipped with a Varian Cary single cell Peltier accessory controlled by a computer. Fluorescence measurements were performed using a Varian Cary Eclipse fluorometer. To minimize reabsorption effects, only solutions with absorbance below 0.1 were used and fluorescence measurements were obtained above the excitation wavelength. Fluorescence intensities were always corrected for dilution.

EPR spectra were recorded in DMSO at room temperature and in frozen solution at 100K using an X-band (9 GHz) Bruker ELEXYS spectrometer equipped with a variable temperature unit. The samples were prepared by dissolution of the compound in dried DMSO and placed in a capillary which was placed in a quartz tube.

Results and Discussion

Synthesis and characterization of 1,8-naphthalimide-modified 3,4-HPO (N-3,4-HPO)

The precursor of the chemosensing ensemble, 4-bromo-1,8-naphthalimide **3** (Scheme 1), was synthesized by condensation of 1,8-naphthalic anhydride **1** with an excess of *N,N*-dimethylethylenediamine **2**, left under reflux in ethanol for 4 hours. Then, in order to prepare

the protected form of ligand **N-3,4-HPO** (derivative **5**, Scheme 1), the Buchwald–Hartwig reaction was carried out by adding 4-bromo-1,8-naphthalimide **3** and 1,6-dimethyl-2-aminomethyl-3-benzyloxy-4-pyridinone **4**,²⁴ in the presence of Pd(OAc)₂ as precatalyst, 2,2'-bis(diphenylphosphanyl)-1,1'-binaphthyl (BINAP) as ligand and *t*-BuOK as base, in DMF, using conventional heating procedure (oil bath, 4 hours of reflux). After evaporation of the solvent, the reaction components were purified by preparative TLC using a mixture of chloroform/methanol (9:1) and characterized by NMR. Following this protocol, derivative **5** was obtained in only 10% of yield (approximately 80% of the starting naphthalimide was recovered) while a by-product was also isolated. This by-product was identified as corresponding to *N*-(dimethylamino)ethyl-4-dimethylamino-1,8-naphthalimide resulting from the reaction of 4-bromo-1,8-naphthalimide **3** with dimethylamine. In fact, DMF has been used as source of dimethylamine in a big number of substitution reactions and it has been speculated that the formation of dimethylamine arises from the decomposition of DMF and happens when the solvent is heated during long periods.^{25,26} In order to confirm this behaviour of DMF, we carried out the reaction of 4-bromo-1,8-naphthalimide **3** in DMF reflux for ca. 10 hours, and obtained exclusively *N*-(dimethylamino)ethyl-4-dimethylamino-1,8-naphthalimide in 10% yield (approximately 90% of the starting naphthalimide was recovered unchanged).

In order to improve the reaction outcome to synthesize **5**, to the detriment of the synthesis of *N*-(dimethylamino)ethyl-4-dimethylamino-1,8-naphthalimide, some modifications were performed on the synthetic procedure. Microwave-assisted synthesis was used as an alternative to the traditional oil bath in order to obtain the desired compound **5** in good yield and the results showed that the reaction time was considerably shorter thus indicating that an improved synthetic protocol is possible. Therefore, in a monomode reactor, under closed-vessel conditions (130°C, 4 min), the reaction of **3** and a 2-fold excess of **4** was performed in the presence of Pd(OAc)₂, BINAP and *t*-BuOK, in DMF. After chromatographic purification, the yield of formation of derivative **5** was significantly improved to 64%. This result shows that, since the reaction time was significantly reduced to 4 min, the degradation of DMF was minimized and, consequently, the side-reaction of dimethylamine resulting from DMF degradation was no longer observed.

The benzyl protecting group of **5** was removed with BCl₃ in dichloromethane, under argon atmosphere, affording the expected dihydrochloride salt of ligand **N-3,4-HPO** in 73% of yield.

NMR spectroscopy

The ligand **N-3,4-HPO** was isolated as +2 charged dihydrochloride salt; one charge is located in the nitrogen atom of the dimethylethylenediamine arm and the other is placed in the nitrogen atom of the dihydroxypyridinium residue.

This is elucidated in the ^1H NMR spectrum performed in DMSO-d_6 by the resonance of the following signals: (i) the multiplet at 3.40-3.42 ppm, corresponding to $^+\text{NH}(\text{CH}_3)_2\text{CH}_2\text{CH}_2$; (ii) the doublet at 2.87 ppm, corresponding to $^+\text{NH}(\text{CH}_3)_2\text{CH}_2\text{CH}_2$ and (iii) the broad singlet at 9.97 ppm assigned to $^+\text{NH}(\text{CH}_3)_2\text{CH}_2\text{CH}_2$. The assignments of the ^{13}C NMR spectrum have been achieved on the basis of HSQC and HMBC experiments. The resonance peaks at 42.6 and 54.8 ppm were assigned to $^+\text{NH}(\text{CH}_3)_2\text{CH}_2\text{CH}_2$ and $^+\text{NH}(\text{CH}_3)_2\text{CH}_2\text{CH}_2$ and these values are consistent with the presence of the charge in the nitrogen atom of the dimethylethylenediamine arm. On the other hand, the singlet corresponding to the resonance of H-5' proton, undergoes a downfield shift to 6.97 ppm, as well as the doublet corresponding to CH_2NH protons, which undergo a downfield shift to 5.02 ppm. Both H-5' and CH_2NH showed strong HMBC correlation with a signal at 143.2 ppm assigned as C-3' (C-OH). Also H-5' showed HMBC correlation with a signal at 160.0 ppm assigned to C-4' (C-OH). These values are in close agreement with chemical shifts values found for other (3,4-HPO)s, confirming that the compound was isolated in the dihydroxypyridinium form.^{23a}

Similar results were obtained when D_2O was used as solvent; in this case a few drops of DCl were added to the NMR tube in order to completely dissolve the compound in D_2O . Under these conditions $^+\text{NH}(\text{CH}_3)_2\text{CH}_2\text{CH}_2$ and $^+\text{NH}(\text{CH}_3)_2\text{CH}_2\text{CH}_2$ appear at 44.3 and 56.4 ppm, C-3' at 143.8 ppm and C-4' at 160.0 ppm, confirming the presence of the +2 charged dihydrochloride salt.

All recorded spectra are provided in supplementary information available.

Electronic spectroscopy

The absorption and fluorescence properties of **N-3,4-HPO** were studied in the UV-Visible region and compared with those of its precursors, 1,8-naphthalic anhydride (**1**) and 4-bromo-1,8-naphthalimide (**3**) (formulae in Scheme 1). The spectra obtained in DMSO are shown in Figures 3a and 3b and those obtained in MOPS buffer solution in Figures 4a and 4b. The compounds are all soluble in DMSO and concentrated solutions in DMSO can be successfully dissolved in buffer solution to be further used in cellular studies. As illustrated in Figure 3a compounds **1** and **3** exhibit quite similar spectra and show bands at 340 and 343 nm,

characteristic of the $\pi \rightarrow \pi^*$ transitions of the π systems in the naphthalene rings. The similarity of the two spectra is indicative that the conversion of the 4-bromo-1,8-naphthalic anhydride in 4-bromo-1,8-naphthalimide did not significantly change the charge distribution in the fluorophore.

The spectrum of **N-3,4-HPO** exhibits two sets of bands, one in the range of 281-290 nm, which corresponds to $\pi \rightarrow \pi^*$ transitions of the π system of the 3,4-HPO ligand and the other band centred at 437 nm which corresponds to $\pi \rightarrow \pi^*$ transitions of the π systems of the naphthalimide fluorophore. The replacement of the bromine group in position 4 of the fluorophore by an amino group or a derivative significantly changes the charge distribution through an ICT mechanism. The spectra obtained in a buffer solution at pH 7.4 (Figure 4a) are very similar to those in DMSO with a slight deviation in the values of λ_{max} as expected for a different solvent. The data obtained is in agreement with the values reported in the literature for similar compounds.²⁷⁻²⁹ The values of λ_{max} and of the molar extinction coefficients of the three compounds are registered in Table 1. The values obtained are close to those described in literature for similar compounds²⁷⁻²⁹ and the usual 10 fold decrease in the value of the molar extinction coefficient that results from the introduction of the amino group in position 4 of the naphthalimide fluorophore is also observed for the new compound **N-3,4-HPO**.

Analysis of the fluorescence spectra of compounds **1**, **3**, and **N-3,4-HPO**, depicted in Figures 3b and 4b, shows that compounds **1** and **3** are not fluorescent in DMSO while compound **N-3,4-HPO** exhibits an emission band centred at *ca* 536 nm which is indicative of the modification of the fluorescent properties of compound **3** upon replacement of the bromine atom by the amino group of the 3,4-HPO residue. In buffer solution at pH=7.4 (Fig. 4b) we observed that 1,8-naphthalic anhydride (**1**) is not fluorescent at all and compound **3** exhibits a very weak emission at 411 nm. Compound **N-3,4-HPO** exhibits an emission band centred at *ca* 536 nm.

Considering the potential application of the new compound in biological media the measurements of fluorescence quantum yield (ϕ_f) were performed in NaOH 0.1 M and MOPS buffer (I=0.1M NaCl, pH 7.4) at 25°C using fluorescein as standard.³⁰ The results are registered in Table 2 and we observed that for compound **N-3,4-HPO** an hypochromic displacement occurs when the pH is lowered to 7.4, thus indicating the sensitivity of the probe to pH variation in that range. Also, the results illustrate that at pH=7.4 the value of the fluorescence quantum yield in MOPS buffer is higher than that in NaOH.

Speciation and evaluation of fluorescence properties of N-3,4-HPO at variable pH

Considering the building molecular fragments of **N-3,4-HPO** and that the compound is isolated in the form of a dichloride salt, it is expected that the compound suffers deprotonation upon dissolution in water. Absorption and fluorescence properties of **N-3,4-HPO** in aqueous solution were studied at variable pH in the range 1.5-10.5. The absorption spectra obtained are displayed in Figure 5 and its analysis show that more than one species is present as pH is increased and that the spectral peaks are shifted in wavelength and exhibit variable intensity. Absorption spectra show a decrease in the maximum of absorbance and a bathochromic shift of the ICT band with the increase of pH. The result is similar to other 4-amino-1,8-naphthalimide containing pH dependent units.^{32,33} The analysis of the data collected with the program HypSpec³⁴ is consistent with the presence of four species and allowed the determination of three pK_a values which are registered in Table 3.

Considering the values of acidity constants reported for 3,4-HPO derivatives, which do not significantly change with the substituents of the heterocyclic ring and are centred at $pK_{a1} \sim 3.5$ and $pK_{a2} \sim 9.3$,³⁵ and those of tertiary amines ($pK_a \sim 10$),³⁶ the formulae of the four species in which **N-3,4-HPO** may be present are indicated in Scheme 2. The corresponding speciation diagram is depicted in Figure 6. The diagram is indicative that at physiological pH conditions the species H_2L^+ is predominant and a smaller amount of the neutral form is also present.

Fluorescence spectra of **N-3,4-HPO** obtained in the range $4 < \text{pH} < 10$ are displayed in Figure 7. The spectra clearly show that the fluorescence intensity diminishes as pH increases and is quenched at above pH equal to 9. From the speciation diagram it can be perceived that at pH 9 the neutral species HL, in which the terminal aliphatic amino group is deprotonated, is the predominant one.

The fluorescence quenching observed at $\text{pH} > 9$ is attributed to a PET process resulting from deprotonation of the amino group (Scheme 3). The terminal aliphatic amino group attached to the 4-amino-1,8-naphthalimide platform acts as a quencher and a photo induced electron transfer process occurs from the lone electron pair of the amino group to the acceptor 1,8-naphthalimide, making the probe weakly fluorescent.

At physiological pH conditions the fluorescent species H_2L^+ is predominant and a smaller amount of the non-fluorescent neutral form is also present.

The protonation of the amino group diminishes the PET effect and leads to restoration of the fluorescence of the 4-amino-1,8-naphthalimide fluorophore at lower pH values. Hence, a marked increase in emission intensity was observed at low pH.³⁷

Interaction of N-3,4-HPO with Fe³⁺, Cu²⁺ and Zn²⁺

Compound **N-3,4-HPO** includes a 3,4-HPO bidentate unit and consequently formation of complexes of type FeL₃, CuL₂ and ZnL₂ is expected.¹⁶ The affinity of 3,4-HPO ligands towards M³⁺ and M²⁺ is well documented in the literature and the stability constants (log β₃ and log β₂) are high and in the range 35.0 < log β₃ < 37.0 for FeL₃ complexes, 17.2 < log β₂ < 19.0 for CuL₂ complexes and 13.2 < log β₂ < 13.7 for ZnL₂ complexes.^{16,22d} Also, it has been shown that the values of protonation constants of 3,4-HPO and the corresponding values of stability constants for a particular metal ion do not differ significantly with alteration of the substituents on the pyridinone ring.¹⁶

Evidence of the interaction of compound **N-3,4-HPO** with Fe³⁺ was assessed, in DMSO and MOPS buffer, by inspection of the electronic spectra of the ligand in the presence of variable concentration of Fe³⁺ and for Cu²⁺ by analysis of the corresponding EPR spectra at RT and 100K obtained also in DMSO.

In order to judge the use of the new compound **N-3,4-HPO** to sense Fe³⁺, Cu²⁺ and Zn²⁺, the interaction of **N-3,4-HPO** with Fe³⁺, Cu²⁺ and Zn²⁺ was also investigated by examining the variations observed in the fluorescence spectra of solutions of the probe in MOPS buffer upon the addition of increasing amounts of the three metal ions.

The absorption and emission spectra of compound **N-3,4-HPO** for a 3:1 ligand:iron(III) ratio obtained in DMSO, are shown in in Figures 8a and 8b, respectively. The absorption spectra clearly show a shift in the ICT band characteristic of the naphthalimide fluorophore and the appearance of a new broad and much less intense band centred at *ca* 550 nm characteristic of formation of an iron(III) complex. Spectra obtained for 2:1 and 1:1 ligand : iron(III) ratios are provided as supplementary information (Figure S1 in supplementary information). The fluorescence spectra obtained for the same solutions are indicative that the fluorescence quenching occurs in the presence of Fe³⁺ and that the effect is concentration dependent. Considering that compound **N-3,4-HPO** is isolated in the form of a dichloride salt and that the NMR spectrum in DMSO confirms that the amino group in the imide position of the naphthalimide fluorophore is protonated, we conclude that fluorescence quenching is the

result of metal ion coordination to the 3,4-HPO unit, since in DMSO the deprotonation of the amino group does not occur and consequently the PET effect observed in aqueous solution is not active.

The absorption and emission spectra of a solution of **N-3,4-HPO** in MOPS buffer, upon addition of increasing amounts of Fe^{3+} are depicted in (Figures 9a and 9b). In figure 9a it is clearly shown that as the concentration of Fe^{3+} is raised the intensity of the bands at *ca* 320-370 nm and the ICT absorption band at $\lambda_{max}=439$ nm decreases. Also, the maximum of the ICT band is shifted to longer wavelength and a less intense band emerges at *ca* 525 nm. These spectral changes are a consequence of coordination of the pyridinone unit to Fe^{3+} and are typical of naphthalimide based probes for sensing cations and anions.^{38,39} In Figure 9b the fluorescence spectra of a solution of **N-3,4-HPO** in MOPS buffer upon addition of increasing amounts of Fe^{3+} are displayed. The spectra show that the intensity of the fluorescence is diminished as the concentration of Fe^{3+} is raised and the quenching of fluorescence is *ca* 92% at a metal:ligand ratio of 1:3. The quenching is assigned to the formation of the *tris* iron(III) complex with the ligand **N-3,4-HPO** (Scheme 4). In the presence of Cu^{2+} and Zn^{2+} the fluorescence of the ligand is also quenched is *ca* 88% for Cu^{2+} and *ca* 91% for Zn^{2+} at a metal:ligand ratio of 1:2. (Figures S2 and S3 in supplementary information)

Confirmation of the coordination of Cu^{2+} with ligand **N-3,4-HPO** is provided by the EPR spectra obtained in DMSO at RT and 100K and shown in (Figures 10a (RT) and 10b (100K)). The spectrum at RT is well resolved and characteristic of one unpaired electron system, $S=1/2$, interacting with a copper nucleus ($I=3/2$). The spectrum obtained at 100K is typical of a copper (II) complex with a rhombic distorted geometry. EPR spectra of copper(II) complexes with N-alkyl-3,4-HPOs are generally characterized by two *g* values and characteristic of square planar complexes with slight distortions in the equatorial plane.^{23b} In the case of ligand **N-3,4-HPO** the spectrum shows a higher degree of anisotropy thus indicating the lower symmetry of the complex which is induced by the nature of the ligand.

Figure 11 shows the structure of the copper(II) complex of ligand **N-3,4-HPO** obtained with the software ChemBio3D[®] Ultra (http://www.cambridgesoft.com/Ensemble_for_Chemistry/ChemBio3D/Default.aspx), after energy minimization. The structure clearly illustrates the distortion induced by the functionalization of the 3,4-HPO unit with the naphthalimide fluorophore.

Conclusions

The conjugation of a 1,8-naphthalimide platform with a 3-hydroxy-4-pyridinone bidentate ligand gave rise to a new fluorescent probe, **N-3,4-HPO**, which is very soluble in water. The compound exhibits pH dependent spectroscopic properties that allowed the determination of three acidity constants. Moreover, the fluorescence intensity of the probe decreases as pH is increased and is *off* above pH equal to 9. This effect is assigned to a PET process induced by deprotonation of the amino group of the fluorescent platform. To improve the possibility of application of this type of probe in cellular media it would be desirable to replace the imide substituent with other groups that enhance water solubility but produce higher fluorescence intensity at physiological pH conditions.

The fluorescence intensity of compound, **N-3,4-HPO**, is also quenched in the presence of variable concentration of Fe^{3+} , Cu^{2+} and Zn^{2+} and the effect is assigned to formation of the corresponding metal ion complexes. As a drawback, the fluorescent probe was not found to be selective to any of the three metal ions although it allows monitoring Cu^{2+} using EPR spectroscopy at room temperature.

Acknowledgments

This work was supported by Fundação para a Ciência e a Tecnologia through projects PTDC/QUI/67915/2006 and PEst-C/EQB/LA0006/2011. T. Moniz also thanks FCT the PhD grant (SFRH/BD/79874/2011). We thank Dr. Andrea Carneiro from CeNTI, V.N. Famalicão, for making available the CEM Discover microwave reactor. The Bruker Avance II 400 spectrometer is part of the National NMR network and was purchased under the framework of the National Programme for Scientific Re-equipment, contract REDE/1517/RMN/2005, with funds from POCI 2010 (FEDER) and (FCT).

References

- [1] Grynkiewicz G, Poenie M, Tsien RY. A new generation of Ca^{2+} indicators with greatly improved fluorescence properties. *J Biol Chem* 1985; 260: 3440-3450.
- [2] Tsien RY. New calcium indicators and buffers with high selectivity against magnesium and protons: Design, synthesis, and properties of prototype structures. *Biochem* 1980; 19: 2396-2404.
- [3] Han J, Burgess K. Fluorescent Indicators for Intracellular pH. *Chem Rev* 2010; 110: 2709-2728.
- [4] (a) Xu Z, Yoon J, Spring DR. Fluorescent chemosensors for Zn^{2+} . *Chem Soc Rev* 2010; **39**: 1996-2006. (b) Nolan EM, Lippard SJ. Tools and Tactics for the Optical Detection of Mercuric Ion. *Chem Rev* 2008; 108: 3443-3480.
- [5] (a) Razgulin A, Ma N, Rao J. Strategies for in vivo imaging of enzyme activity: an overview and recent advances. *Chem Soc Rev* 2011; 40, 4186-4216. (b) Serim S, Haedke U, Verhelst SHL. Activity-based probes

- for the study of proteases: Recent advances and developments. *Chem Med Chem* 2012, **7**, 1146-1159. (c) Mizukami S. Development of Molecular Imaging Tools to Investigate Protein Functions by Chemical Probe Design. *Chem Pharm Bull* 2011; **59**: 1435-1446.
- [6] (a) Miller EW, Chang CJ. Fluorescent probes for nitric oxide and hydrogen peroxide in cell signaling. *Curr Opin Chem Biol* 2007; **11**: 620-625. (b) Chen X, Tian X, Shin I, Yoon J. Fluorescent and luminescent probes for detection of reactive oxygen and nitrogen species. *Chem Soc Rev* 2011; **40**: 4783-4804. (c) Hyman LM, Frank KJ. Probing oxidative stress: Small molecule fluorescent sensors of metal ions, reactive oxygen species, and thiols. *Coord Chem Rev* 2012; **256**: 2333-2356.
- [7] (a) Nagano T. Development of fluorescent probes for bioimaging applications. *Proc Jpn Acad Ser B* 2010; **86**: 837-847. (b) Ueno T, Nagano T. Fluorescent probes for sensing and imaging. *Nature Methods* 2011; **8**, 642-645.
- [8] (a) Bissell RA, de Silva AP, Gunaratne HQN, Lynch PLM, Maguire GEM, Sandanayake KRAS. Molecular fluorescent signalling with 'fluor-spacer-receptor' systems: Approaches to sensing and switching devices via supramolecular photophysics. *Chem Soc Rev* 1992; **21**: 187-195. (b) de Silva AP, Gunaratne HQN, Gunnlaugsson T, Huxley AJM, McCoy CP, Rademacher JT, Rice TE. Signaling recognition events with fluorescent sensors and switches. *Chem Rev* 1997; **97**: 1515-1566. (c) Gunnlaugsson T, Davis AP, O'Brien JE, Glynn M. Synthesis and photophysical evaluation of charge neutral thiourea or urea based fluorescent PET sensors for bis-carboxylates and pyrophosphate. *Org Biomol Chem* 2005; **3**: 48-56. (d) dos Santos CMG, Glynn M, McCabe T, Seixas de Melo JS, Burrows HD, Gunnlaugsson T. Synthesis, structural and photophysical evaluations of urea based fluorescent PET sensors for anions. *Supramol Chem* 2007; **20**: 407-418.
- [9] (a) de Silva AP, Rupasinghe RADD. A new class of fluorescent pH indicators based on photo-induced electron transfer. *J Chem Soc Chem Commun* 1985: 1669-1670. (b) de Silva AP, de Silva SA. Fluorescent signalling crown ethers; 'switching on' of fluorescence by alkali metal ion recognition and binding in situ. *J Chem Soc Chem Commun* 1986: 1709-1710. (c) Huston ME, Haider KW, Czarnik AW. Chelation-enhanced fluorescence in 9,10-bis(TMEDA)anthracene [33]. *J Am Chem Soc* 1988; **110**: 4460-4462. (d) Czarnik AW. Chemical communication in water using fluorescent chemosensors. *Acc Chem Res* 1994; **27**: 302-308.
- [10] (a) Gunnlaugsson T, Glynn M, Tocci (née Hussey) GM, Kruger PE, Pfeffer FM. Anion recognition and sensing in organic and aqueous media using luminescent and colorimetric sensors. *Coord Chem Rev* 2006, **250**: 3094-3117. (b) Duke RM, Veale EB, Pfeffer FM, Kruger PE, Gunnlaugsson T. Colorimetric and fluorescent anion sensors: an overview of recent developments in the use of 1,8-naphthalimide-based chemosensors. *Chem Soc Rev* 2010; **39**: 3936-3953. (c) Qian X, Xiao Y, Xu Y, Guo X, Qiana J, Zhua W. 'Alive' dyes as fluorescent sensors: fluorophore, mechanism, receptor and images in living cells. *Chem Commun* 2010; **46**: 6418-6436.
- [11] de Silva AP, Gunaratne HQN, Lynch PLM, Patty AJ, Spence GL. Luminescence and charge transfer. part 3. The use of chromophores with ICT (internal charge transfer) excited states in the construction of fluorescent PET (photoinduced electron transfer) pH sensors and related absorption pH sensors with aminoalkyl side chains. *J Chem Soc Trans 2*; 1993: 1611-1616.
- [12] Oelgemöller M, Kramer WH. Synthetic photochemistry of naphthalimides and related compounds. *J Photochem Photobiol C: Photochem Rev* 2010; **11**: 210-244.

[13] For Cu^{2+} please see (a) Xu Z, Xiao Y, Qian X, Cui J, Cui D. Ratiometric and Selective Fluorescent Sensor for Cu(II) Based on Internal Charge Transfer (ICT). *Org Lett* 2005; **7**: 889-892. (b) Xu Z, Qian X, Cui J. Colorimetric and ratiometric fluorescent chemosensor with a large red-shift in emission: Cu(II)-only sensing by deprotonation of secondary amines as receptor conjugated to naphthalimide fluorophore. *Org Lett* 2005; **7**: 3029-3032. (c) Huang J, Xu Y, Qian X. A colorimetric sensor for Cu^{2+} in aqueous solution based on metal ion-induced deprotonation: deprotonation/protonation mediated by Cu^{2+} -ligand interactions. *Dalton Trans* 2009: 1761-1766. (d) Huang J, Xu Y, Qian X. A red-shift colorimetric and fluorescent sensor for Cu^{2+} in aqueous solution: unsymmetrical 4,5-diaminonaphthalimide with N-H deprotonation induced by metal ions. *Org Biomol Chem* 2009; **7**: 1299-1303. (e) Singh N, Kaur N, McCaughan B, Callan JF. Ratiometric fluorescent detection of Cu(II) in semi-aqueous solution using a two-fluorophore approach. *Tetrahedron Lett* 2010; **51**: 3385-3387. (f) Sahin O, Yilmaz M. Synthesis and fluorescence sensing properties of a new naphthalimide derivative of calix[4]arene. *Tetrahedron Lett* 2012; **53**: 2319-2324. (g) Liu Z, Zhang C, Wang X, He W, Guo Z. Design and synthesis of a ratiometric fluorescent chemosensor for Cu(II) with a fluorophore hybridization approach. *Org Lett* 2012; **14**: 4378-4381.

For Zn^{2+} please see (a) Gunnlaugsson T, Lee TC, Parkesh R. A highly selective and sensitive fluorescent PET (photoinduced electron transfer) chemosensor for Zn(II). *Org Biomol Chem* 2003; **1**: 3265-3267. (b) Parkesh R, Lee TC, Gunnlaugsson T. Highly selective 4-amino-1,8-naphthalimide based fluorescent photoinduced electron transfer (PET) chemosensors for Zn(II) under physiological pH conditions. *Org Biomol Chem* 2007; **5**: 310-317.

[14] For Hg^{2+} please see (a) Guo X, Qian X, Jia L. A highly selective and sensitive fluorescent chemosensor for Hg^{2+} in neutral buffer aqueous solution. *J Am Chem Soc* 2004; **126**: 2272-2273. (b) Liu B, Tian H. A selective fluorescent ratiometric chemodosimeter for mercury ion. *Chem Commun* 2005: 3156-3158. (c) Wang J, Qian X. Two regioisomeric and exclusively selective Hg(II) sensor molecules composed of a naphthalimide fluorophore and an *o*-phenylenediamine derived triamide receptor. *Chem Commun* 2006: 109-111. (d) He C, Zhu W, Xu Y, Chen T, Qian X. Trace mercury (II) detection and separation in serum and water samples using a reusable bifunctional fluorescent sensor. *Anal Chim Acta* 2009; **651**: 227-233. (e) Dai H, Xu H. A water-soluble 1,8-naphthalimide-based 'turn on' fluorescent chemosensor for selective and sensitive recognition of mercury ion in water. *Bioorg Med Chem Lett* 2011; **21**: 5141-5144. (f) Meng Q, Zhang X, He C, Zhou P, Su W, Duan C. A hybrid mesoporous material functionalized by 1,8-naphthalimide-base receptor and the application as chemosensor and absorbent for Hg^{2+} in water. *Talanta* 2011; **84**: 53-59. (g) Fang CL, Zhou J, Liu XJ, Cao ZH, Shangguan DH. Mercury(II)-mediated formation of imide-Hg-imide complexes. *Dalton Trans* 2011; **40**: 899-903. (h) Yang R, Guo X, Wang W, Zhang Y, Jia L. Highly Selective and Sensitive Chemosensor for Hg^{2+} Based on the Naphthalimide Fluorophore. *J Fluoresc* 2012; **22**: 1065-1071. (i) Li CY, Xu F, Li YF, Zhou K, Zhou Y. A fluorescent chemosensor for Hg^{2+} based on naphthalimide derivative by fluorescence enhancement in aqueous solution. *Anal Chim Acta* 2012; **717**: 122-126.

For Pd^{2+} please see: Duan L, Xu Y, Qian X. Highly sensitive and selective Pd^{2+} sensor of naphthalimide derivative based on complexation with alkynes and thio-heterocycle. *Chem Commun* 2008: 6339-6341.

[15] (a) Hanaoka K, Muramatsu Y, Urano Y, Terai T, Nagano T. Design and synthesis of a highly sensitive off-on fluorescent chemosensor for zinc ions utilizing internal charge transfer. *Chem Eur J* 2010; **16**: 568-572. (b) Xu Z, Han SJ, Lee C, Yoon J, Spring DR. Development of off-on fluorescent probes for heavy and

- transition metal ions. *Chem Commun* 2010; 46: 1679-1681. (c) Wang H, Yang L, Zhang W, Zhou Y, Zhao B, Li X. A colorimetric probe for copper(II) ion based on 4-amino-1,8-naphthalimide. *Inorg Chim Acta* 2012; 381: 111-116.
- [16] Burgess J, Rangel M. Hydroxypyranones, hydroxypyridinones and their complexes. *Adv Inorg Chem* 2008; 60: 167-243.
- [17] (a) Cohen SM, O'Sullivan B, Raymond KN. Mixed hydroxypyridinonate ligands as iron chelators. *Inorg Chem* 2000; 39: 4339-4346. (b) Xu J, O'Sullivan B, Raymond KN. Hexadentate hydroxypyridonate iron chelators based on TREN-Me-3,2-HOPO: variation of cap size. *Inorg Chem* 2002; 41: 6731-6742.
- [18] Raymond KN, Xu J. US Patent. 5 624 901, 1997.
- [19] (a) Santos MA, Marques SM, Chaves S. Hydroxypyridinones as "privileged" chelating structures for the design of medicinal drugs. *Coord Chem Rev* 2012; 256: 240-259. (b) Rodríguez-Rodríguez C, Telpoukhovskaia M, Orvig C. The art of building multifunctional metal-binding agents from basic molecular scaffolds for the potential application in neurodegenerative diseases. *Coord Chem Rev* 2012; 256: 2308-2332. (c) Santos MA. Hydroxypyridinone complexes with aluminium. *In vitro/vivo* studies and perspectives. *Coord Chem Rev* 2002; 228: 187-203.
- [20] (a) Ma Y, Luo W, Quinn PJ, Liu Z, Hider RC. Design, Synthesis, Physicochemical Properties, and Evaluation of Novel Iron Chelators with Fluorescent Sensors. *J Med Chem* 2004; 47: 6349-6362. (b) Katoh A, Ogino K, Saito R. Synthesis of new 3-hydroxy-4(1H)-pyridinone directly attached to quinoxaline and its fluorescence property upon complexation to metal ions. *Heterocycles* 2005; 65: 2195-2201. (c) Fakhri S, Podinovskaia M, Kong X, Collins HL, Schaible UE, Hider RC. Targeting the Lysosome: Fluorescent Iron(III) Chelators To Selectively Monitor Endosomal/Lysosomal Labile Iron Pools. *J Med Chem* 2008; 51: 4539-4552. (d) Fakhri S, Podinovskaia M, Kong X, Schaible UE, Collins HL, Hider RC. Monitoring intracellular labile iron pools: A novel fluorescent iron(III) sensor as a potential non-invasive diagnosis tool. *J Pharm Sci* 2009; 98: 2212-2226.
- [21] Sahoo SK, Sharma D, Bera RK, Crisponi G, Callan JF. Iron(III) selective molecular and supramolecular fluorescent probes. *Chem Soc Rev* 2012; 41: 7195-7227.
- [22] a) Fernandes SS, Nunes A, Gomes AR, de Castro B, Hider RC, Rangel M, Appelberg R, Gomes MS. Identification of a new hexadentate iron chelator capable of restricting the intramacrophagic growth of *Mycobacterium avium*. *Microbes Infect* 2010; 12: 287-294. b) Nunes A, Podinovskaia M, Leite A, Gameiro P, Zhou T, Ma Y, Kong X, Schaible UE, Hider RC, Rangel M. Fluorescent 3-hydroxy-4-pyridinone hexadentate iron chelators: Intracellular distribution and the relevance to antimycobacterial properties. *J Biol Inorg Chem* 2010; 15: 861-877. c) Rangel M, Amorim MJ, Nunes A, Leite A, Pereira E, de Castro B, Sousa C, Yoshikawa Y, Sakurai H. Novel 3-hydroxy-4-pyridinonato oxidovanadium(IV) complexes to investigate structure/activity relationships. *J Inorg Biochem* 2009; 103: 496-502. d) Moniz T, Amorim MJ, Ferreira R, Nunes A, Silva A, Queirós C, Leite A, Gameiro P, Sarmiento B, Remião F, Yoshikawa Y, Sakurai H, Rangel M. Investigation of the insulin-like properties of zinc(II) complexes of 3-hydroxy-4-pyridinones: Identification of a compound with glucose lowering effect in STZ-induced type i diabetic animals. *J Biol Inorg Chem* 2011; 105: 1675-1682.
- [23] a) Silva AMG, Leite A, Andrade M, Gameiro P, Brandão P, Felix V, de Castro B, Rangel M. Microwave-assisted synthesis of 3-hydroxy-4-pyridinone/naphthalene conjugates. Structural characterization and

- selection of a fluorescent ion sensor. *Tetrahedron* 2010; 66: 8544-8550. b) Silva AMG, Leite A, Gonzalez P, Domingues MRM, Gameiro P, de Castro B, Rangel M. Use of a porphyrin platform and 3,4-HPO chelating units to synthesize ligands with N4 and O4 coordination sites. *Tetrahedron* 2011; 67: 7821-7828.
- [24] Liu ZD, Kayyali R, Hider RC, Porter JB, Theobald AE. Design, synthesis, and evaluation of novel 2-substituted 3-hydroxypyridin-4-ones: Structure-activity investigation of metalloenzyme inhibition by iron chelators. *J Med Chem* 2002; 45: 631-639.
- [25] Muzart J. *N,N*-Dimethylformamide: much more than a solvent. *Tetrahedron* 2009; 65: 8313-8323.
- [26] Ding S, Jiao N. *N,N*-dimethylformamide: A multipurpose building block. *Angew Chem Int Ed* 2012; 51: 9226-9237.
- [27] Bojinov VB, Georgiev NI, Nikolov PS. Synthesis and photophysical properties of fluorescence sensing ester- and amidoamine-functionalized 1,8-naphthalimides. *J Photochem Photobiol A: Chem* 2008; 193: 129-138.
- [28] Alexiou MS, Tychopoulos V, Ghorbanian S, Tyman JHP, Brown RG, Brittain PI. The UV-visible absorption and fluorescence of some substituted 1,8-naphthalimides and naphthalic anhydrides. *J Chem Soc Perkin Trans 2* 1990: 837-842.
- [29] Li Z, Yang Q, Chang R, Ma G, Chen M, Zhang W. *N*-Heteroaryl-1,8-naphthalimide fluorescent sensor for water: Molecular design, synthesis and properties. *Dyes Pigm* 2011; 88: 307-314.
- [30] Williams ATR, Winfield SA, Miller JN. Relative fluorescence quantum yields using a Computer-controlled luminescence spectrometer. *Analyst* 1983; 108: 1067-1071.
- [31] Lakowicz JR. Principles of fluorescence spectroscopy. 3 ed. Berlin, Heidelberg: Springer, 2006.
- [32] Tian Y, Su F, Weber W, Nandakumar V, Shumway BR, Jin Y, Zhou X, Holl MR, Johnson RH, Meldrum DR. A series of naphthalimide derivatives as intra and extracellular pH sensors. *Biomaterials* 2010; 31: 7411-7422.
- [33] Niu CG, Zeng GM, Chen LX, Shen GL, Yu RQ. Proton "off-on" behaviour of methylpiperazinyl derivative of naphthalimide: A pH sensor based on fluorescence enhancement. *Analyst* 2004; 129: 20-24.
- [34] Gans P, Sabatini A, Vacca A. Investigation of equilibria in solution. Determination of equilibrium constants with the HYPERQUAD suite of programs. *Talanta* 1996; 43: 1739-1753.
- [35] Queiros C, Amorim MJ, Leite A, Ferreira M, Gameiro P, Castro B, Biernacki K, Magalhães A, Burgess J, Rangel M. Nickel(II) and cobalt(II) 3-hydroxy-4-pyridinone complexes: Synthesis, characterization and speciation studies in aqueous solution. *Eur J Inorg Chem* 2011; 1: 131-140.
- [36] Frenna V, Vivona N, Consiglio G, Spinelli D. Amine basicities in benzene and in water. *J Chem Soc Perkin Trans 2* 1985: 1865-1868.
- [37] Niu CG, Gui XQ, Zeng GM, Yuan XZ. A ratiometric fluorescence sensor with broad dynamic range based on two pH-sensitive fluorophores. *Analyst* 2005; 130: 1551-1556.
- [38] Chaves S, Canário S, Carrasco MP, Mira L, Santos MA. Hydroxy(thio)pyrone and hydroxy(thio)pyridinone iron chelators: Physico-chemical properties and anti-oxidant activity. *J Inorg Biochem* 2012; 114: 38-46.
- [39] Veale EB, Tocci GM, Pfeffer FM, Krugera PE, Gunnlaugsson T. Demonstration of bidirectional photoinduced electron transfer (PET) sensing in 4-amino-1,8-naphthalimide based thiourea anion sensors. *Org Biomol Chem* 2009; 7: 3447-3454.

- [40] Xie L, Xu Y, Wang F, Liu J, Qian X, Cui J. Synthesis of new amonafide analogues via coupling reaction and their cytotoxic evaluation and DNA-binding studies. *Bioorg Med Chem* 2009; 17: 804-810.
- [41] Wan Y, Alterman M, Hallberg A. Palladium-catalyzed amination of aryl bromides using temperature-controlled microwave heating. *Synthesis* 2002; 11: 1597-1600.
- [42] Forgues SF, Lavabre D. Are fluorescence quantum yields so tricky to measure? A demonstration using familiar stationery products. *J Chem Ed* 1999; 76: 1260-1264.
- [43] Albert A, Sergeant EP. *The Determination of Ionization Constants*. 2 ed., Chapman & Hall, London, 1971.
- [44] Alderighi L, Gans P, Ienco A, Peters D, Sabatini A, Vacca A. Hyperquad simulation and speciation (HySS): A utility program for the investigation of equilibria involving soluble and partially soluble species. *Coord Chem Rev* 1999; 184: 311-318.

Highlights

- The conjugation of a naphthalimide with a pyridinone gave a new fluorescent probe.
- The conjugation reaction was successfully achieved by using microwave irradiation.
- Photophysical properties (absorption, fluorescence, quantum yield) were determined.
- Fe(III), Cu(II) and Zn(II) lead to a considerable fluorescence quenching effect.

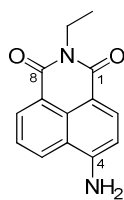


Fig 1. 4-amino-1,8-naphthalimide structure.

ACCEPTED MANUSCRIPT

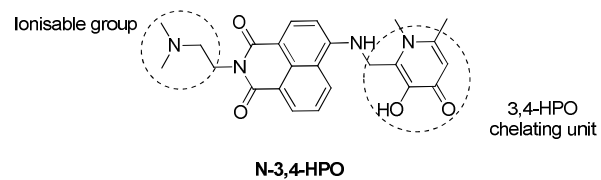


Fig. 2 1,8-Naphthalimide modified 3,4-HPO (**N-3,4-HPO**).

ACCEPTED MANUSCRIPT

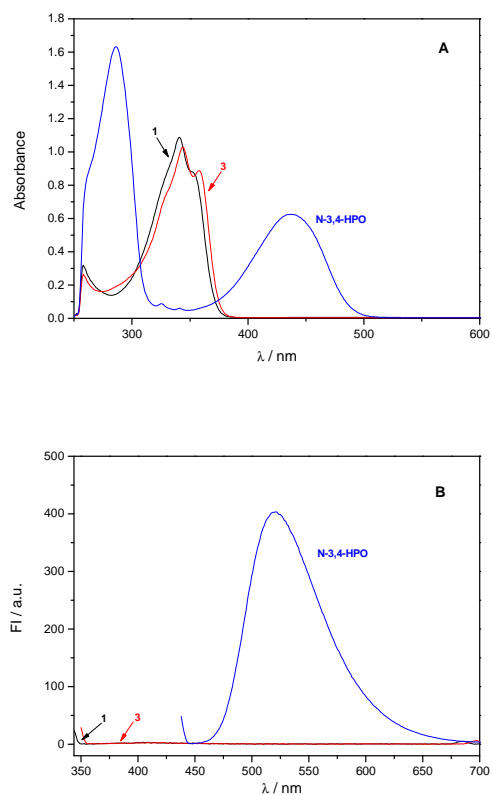


Fig. 3. (A) UV-Vis spectra of 1,8-naphthalic anhydride (**1**) (black line), compound **3** (red line) and N-3,4-HPO (blue line) in DMSO ($T=25^{\circ}\text{C}$) and concentration 7.5×10^{-5} M; (B) Fluorescence spectra of 1,8-naphthalic anhydride (**1**) (black line, $\lambda_{\text{exc}} = 342$ nm, λ_{em} from 344-700 nm), compound **3** (red line, $\lambda_{\text{exc}} = 348$ nm, λ_{em} from 350-700 nm) and N-3,4-HPO (blue line, $\lambda_{\text{exc}} = 437$ nm, λ_{em} from 438-700 nm) in DMSO ($T=25^{\circ}\text{C}$, 600 V, 5 nm slits) and concentration 7.5×10^{-5} M.

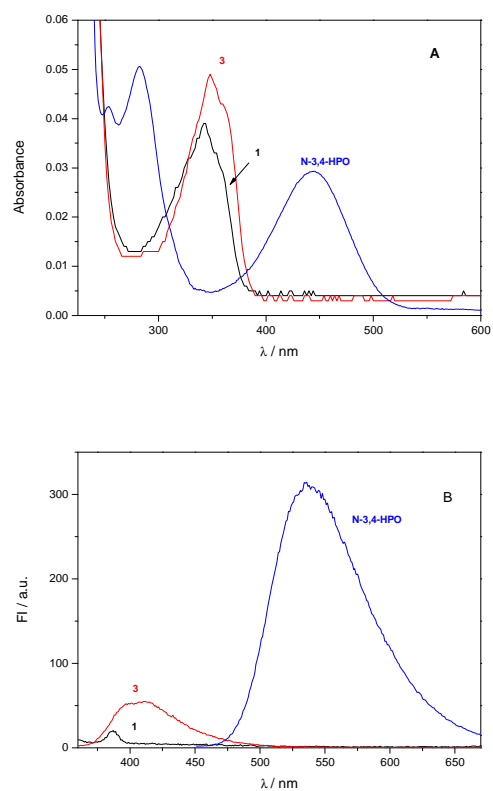


Fig. 4. (A) UV-Vis spectra of 1,8-naphthalic anhydride (**1**) (black line), compound **3** (red line) and **N-3,4-HPO** (blue line) in MOPS ($I=0.1$ M NaCl, pH=7.4, $T=25^\circ\text{C}$) and concentration 3.0×10^{-6} M; (B) Fluorescence spectra of 1,8-naphthalic anhydride (**1**) (in black, $\lambda_{\text{exc}} = 342$ nm, λ_{em} from 344-650 nm), compound **3** (in red, $\lambda_{\text{exc}} = 348$ nm, λ_{em} from 350-650 nm) and **N-3,4-HPO** (in blue, $\lambda_{\text{exc}} = 439$ nm, λ_{em} from 441-650 nm) in MOPS (pH=7.4, $T=25^\circ\text{C}$, 600 V, 5 nm slits) and concentration 3.0×10^{-6} M.

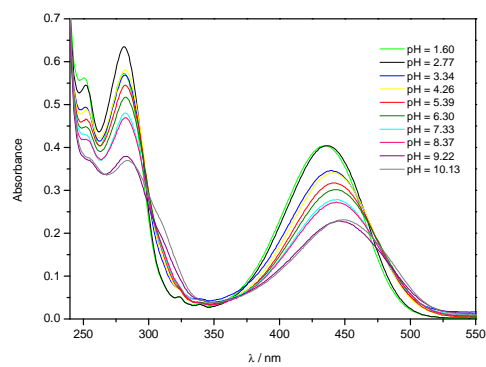


Fig. 5. Absorption spectra of 4.0×10^{-5} M aqueous solution of N-3,4-HPO at variable pH and 25°C.

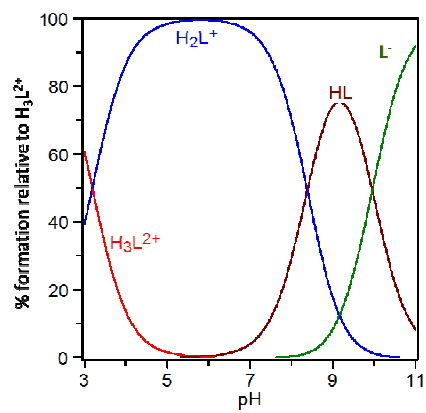


Fig. 6. Speciation diagram of N-3,4-HPO in aqueous solution.

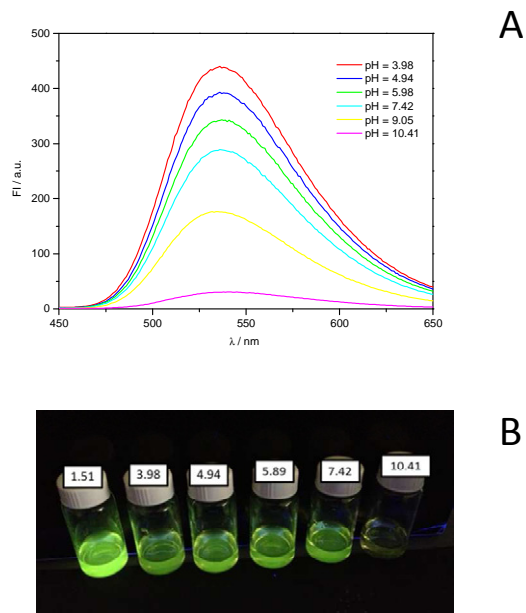


Fig. 7. (A) Fluorescence spectra of **N-3,4-HPO** at pH: 1.5, 4, 5, 6, 7.4, 9 and 10 (λ_{exc} =434 nm, λ_{em} from 441-650 nm; T= 25°C, 590 V, 5 nm slits) and concentration 8.0×10^{-6} M; **(B)** Effect of pH on fluorescent properties of the ligand.

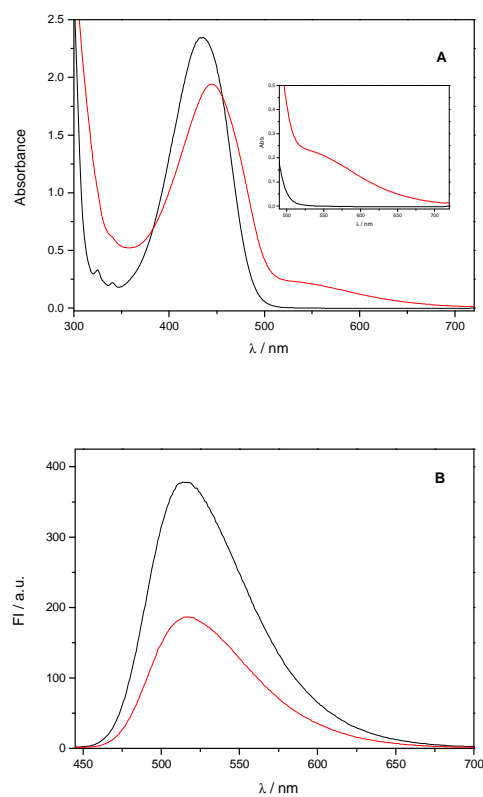


Fig. 8. (A) Absorption spectra of **N-3,4-HPO** at 3.0×10^{-4} M (DMSO, T= 25°C) (black line) and in the presence of Fe^{3+} in a metal:ligand ratio 1:3 (red line [N-3,4-HPO] = 3.0×10^{-4} M); (B) Fluorescence spectra of **N-3,4-HPO** at 2.5×10^{-5} M (DMSO, T= 25°C) (black line) and in the presence of Fe^{3+} in a metal/ligand ratio 1:3 (red line, [N-3,4-HPO] = 7.5×10^{-5} M). All spectra were recorded at $\lambda_{\text{exc}}=437$ nm, $\lambda_{\text{em}}=438-700$ nm, T= 25°C, 550 V, 5 nm slits.

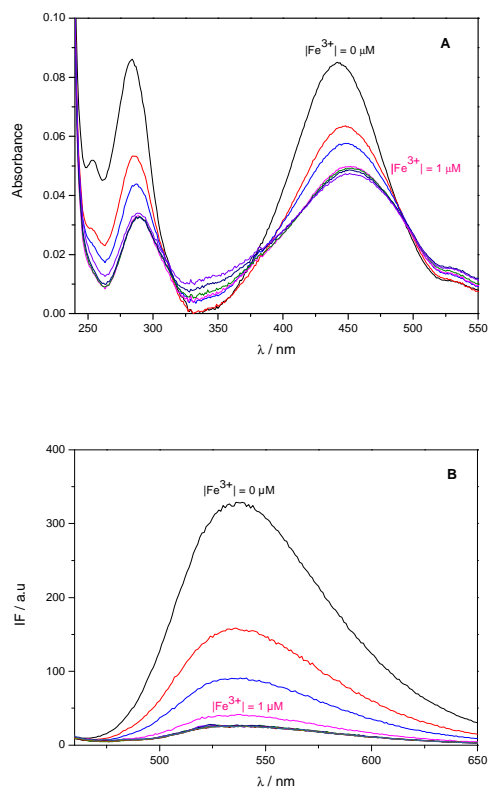


Fig.9. (A) Absorption spectra of N-3,4-HPO at 3.0×10^{-6} M (MOPS buffer, I= 0.1 M NaCl, 25°C, pH=7.4) with increasing concentration of Fe^{3+} ; (B) Fluorescence spectra of N-3,4-HPO at 3.0×10^{-6} M (MOPS buffer, I= 0.1 M NaCl, 25°C, pH=7.4, $\lambda_{exc}=439$ nm) with increasing concentration of Fe^{3+} .

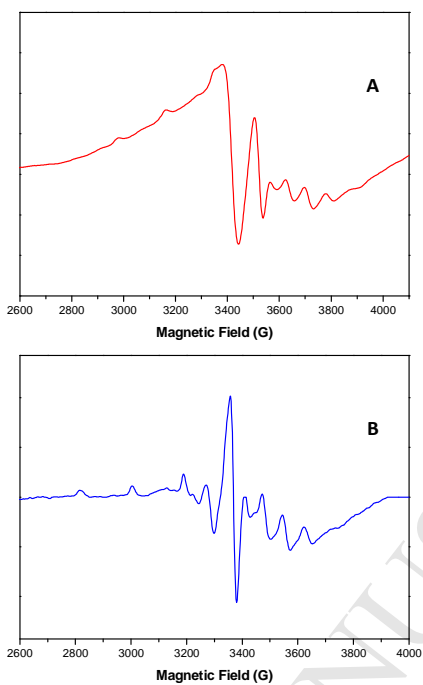


Fig. 10. EPR spectra of the copper(II) complex with ligand N-3,4-HPO obtained in DMSO at (A) room temperature in the following experimental conditions: microwave frequency of 9.450 GHz, microwave power of 20 mW and modulation amplitude of 4 G (B) at 100K in the following experimental conditions: microwave frequency of 9.447 GHz, microwave power of 20 mW and modulation amplitude of 8 G.

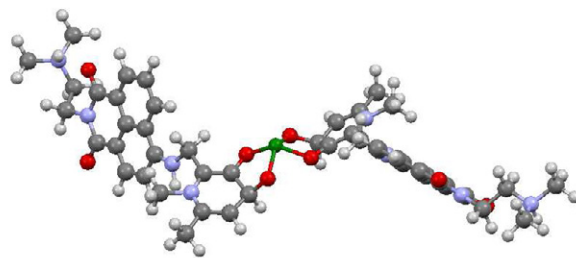
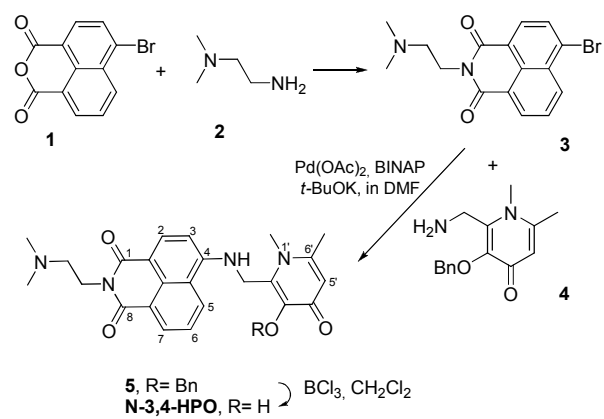
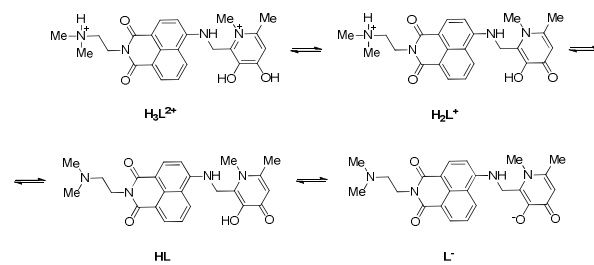


Fig. 11. Structure of the copper(II) complex of ligand N-3,4-HPO obtained with the software ChemBio3D[®] Ultra 12.0, after energy minimization.

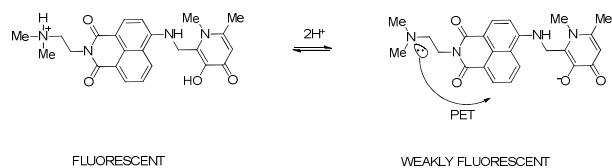
ACCEPTED MANUSCRIPT



Scheme 1 Synthesis of 1,8-naphthalimide-modified 3,4-HPO (**5**) and **N-3,4-HPO**.

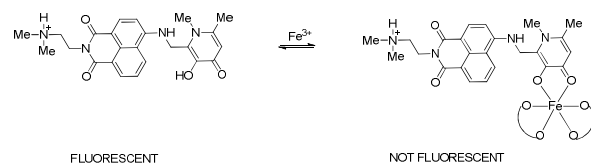


Scheme 2. Proposed dissociation steps of N-3,4-HPO.



Scheme 3 Probe response at variable pH.

ACCEPTED MANUSCRIPT



Scheme 4. Probe response towards Fe^{3+} coordination.

Table 1 - Photophysical properties of compounds **1**, **3** and **N-3,4-HPO** (in MOPS buffer, I=0.1 M NaCl, pH=7.4), and DMSO (T = 25°C, 7.5x10⁻⁵ M).

Compound	Solvent	UV-Vis		Fluorescence
		$\epsilon / \text{mol}^{-1}\text{dm}^3\text{cm}^{-1}$	$\lambda_{\text{max}} / \text{nm}$	$\lambda_{\text{em max}} / \text{nm}$
1	DMSO	1.45×10^4	341	--
	MOPS	1.04×10^5	342	--
3	DMSO	1.37×10^4	344	--
	MOPS	1.41×10^5	348	411
N-3,4-HPO	DMSO	8.35×10^3	437	421
	MOPS	1.47×10^4	439	536

Table 2. Quantum yield (ϕ_f) of compounds **3**, **N-3,4-HPO** and fluorescein in NaOH 0.1 M (pH 14, 25°C) and MOPS (10 mM, I=0.1M NaCl, pH 7.4, 25°C).

Compound	NaOH		MOPS	
	λ_{\max} (nm)	ϕ_f	λ_{\max} (nm)	ϕ_f
Fluorescein	491	0.95 ^(a)	491	0.93
N-3,4-HPO	446	0.04	439	0.12

^(a) Value published in reference 31.

Table 3. Acidic constants of N-3,4-HPO.

pK_{ai}	N-3,4-HPO (H_3L^{2+})
pK_{a1}	3.19 ± 0.02
pK_{a2}	8.38 ± 0.05
pK_{a3}	9.95 ± 0.52